Doping dependence of transport and magnetic properties in $La_{1-x}Ca_xVO_3$

1997 J. Phys.: Condens. Matter 9 7507

(http://iopscience.iop.org/0953-8984/9/35/024)

J. Phys.: Condens. Matter **9** (1997) 7507–7514. Printed in the UK PII: S0953-8984(97)83681-8

Doping dependence of transport and magnetic properties in $La_{1-x}Ca_xVO_3$

K Maiti, N Y Vasanthacharya and D D Sarma†

Solid State and Structural Chemistry Unit, Indian Institute of Science, Bangalore 560012, India

Received 24 April 1997

Abstract. We report temperature dependences of transport and magnetic properties of $La_{1-x}Ca_xVO_3$ controlled by charge carrier doping ($x = 0.0$–0.5). The system exhibits an insulator-to-metal transition concomitant with an antiferromagnetic-to-paramagnetic transition near $x = 0.2$ with increasing substitution. Disorder effects are found to influence the low-temperature transport properties of both insulating and metallic compositions near the critical concentration. At higher temperature resistivity of the metallic compositions has a T^2 dependence close to the critical concentration ($x = 0.2$ and 0.3) and thus provides an example of disordered Fermi liquid behaviour near the Mott transition. In contrast, at larger doping ($x = 0.4$ and 0.5) the resistivity exhibits a $T^{1.5}$ dependence. The molar susceptibility for the metallic samples indicates substantial enhancements due to electron correlation.

The study of metal–insulator (MI) transitions in early transition metal (Ti and V) oxides has attracted a lot of attention in recent times [1–8]. Most of these oxides have the perovskite structure which allows for doping of charge carriers by chemical heterovalent substitutions over a wide range of compositions without breaking the structural network. Moreover, this basic structure type makes it possible to tune various structural parameters, such as the bond angles and bond lengths, which directly affect the bandwidth by altering the intra- and inter-cluster hopping interactions. Thus, it becomes possible to investigate metal–insulator transitions as a function of charge carrier tuning as well as bandwidth (or correlation effects) control.

Two such series of compounds, $La_{1-x}Sr_xVO_3$ and $Y_{1-x}Ca_xVO_3$, related to the present work, have been investigated extensively to date for several values of x [2, 3, 6]. $LaVO_3$ is an antiferromagnetic insulator with Néel temperature around 140 K [9], a charge excitation gap of about 1.1 eV [4] and a distorted perovskite structure [10–15]. Sr substitution drives the system towards the cubic perovskite structure [16] with concomitant doping of holes into the system, thereby driving it to a metallic phase at about 22% hole doping [17], a value very near to the percolation threshold ($x \sim 0.26$). The system remains antiferromagnetic throughout the insulating regime ($x \leqslant 0.2$) and shows paramagnetic susceptibility in the metallic phase [18]. YVO_3 is also an antiferromagnetic insulator with orthorhombically distorted perovskite structure [19]. Here the V–O–V bond angle is lower ($\sim 145^\circ$) than that of $LaVO_3$ ($\sim 158^\circ$) [20] leading to a decreased bandwidth in YVO_3. Ca substitution leads to MI transitions in this system for larger values of x ($x_c \sim 0.5$) compared to the case of $La_{1-x}Sr_xVO_3$ ($x_c \sim 0.22$). This large x_c in YVO_3 rules out the possibility of percolation being an explanation for the MI transition in this system. One possible reason

† Also at Jawaharlal Nehru Centre for Advanced Scientific Research, Bangalore.

0953-8984/97/357507+08$19.50

for this large value for the critical concentration might be the smaller band width in YVO_3 compared to $LaVO_3$ discussed above. This suggests that changing electron correlation effects concomitant with doping variation, also play an important role in these MI transitions; however, it is not possible to separate out the effects arising from the changes in the bandwidth from those due to changing charge carrier concentrations.

In order to address these important issues, we study the transport and magnetic properties of $LaVO_3$ and its Ca substituted compositions, $La_{1-x}Ca_xVO_3$ for various values of x. This system is different from $La_{1-x}Sr_xVO_3$ since the effective ionic radius of Ca^{2+} (1.34 Å) is very close to that of La^{3+} (1.36 Å), in contrast to that of Sr^{2+} (1.44 Å) [21]. The crystal structures of the two end members $LaVO_3$ and $CaVO_3$ are both distorted perovskite type [2, 10–15, 22] with similar V–O–V bond angle ($\sim$160° in $CaVO_3$) [7], while $SrVO_3$ is cubic. Thus, unlike Sr^{2+} substitution, Ca^{2+} substitution in $LaVO_3$ dopes hole states without much change in structure and consequently, in bandwidth. In view of this, it is reasonable to expect that the changes in the transport and magnetic properties in $La_{1-x}Ca_xVO_3$ are more controlled by the tuning of the doping level with comparatively less influence from the changes in the correlation effects, in contrast to the previously studied $La_{1-x}Sr_xVO_3$ and $Y_{1-x}Ca_xVO_3$.

The samples of $La_{1-x}Ca_xVO_3$ ($x = 0.0$, 0.1, 0.2, 0.3, 0.4 and 0.5) have been prepared by taking stoichiometric amounts of predried La_2O_3, $CaCO_3$ and V_2O_5 in appropriate proportions. After calcining at 800 °C for 24 hours, the mixture was reduced at 800 °C for 24 hours in a hydrogen atmosphere and the resulting samples were melted in a dc arc furnace in an inert gas atmosphere. All the samples have been characterized by x-ray powder diffraction (XRD) pattern, which show single phase for all compositions without any change in the structure. The oxygen stoichiometry has been measured thermogravimetrically by heating the samples at 500 °C for about 72 hours in flowing oxygen, thereby converting all V ions to the highest oxidation state of V^{5+}. Thus, we estimate δ to be 0.04, 0.03, 0.04, 0.01, -0.01 and 0.0 in $La_{1-x}Ca_xVO_{3+\delta}$ for $x = 0.0$, 0.1, 0.2, 0.3, 0.4 and 0.5 respectively. The resistivity measurements have been carried out using a dc four-probe resistivity set-up following Van der Pauw's method. The dc magnetic susceptibility measurements have been performed in the temperature range 20–300 K using a Lewis coil force magnetometer at a field of 5 kOe.

We show the resistivity (ρ) of $La_{1-x}Ca_xVO_3$ for $x = 0.0$ and 0.1 as a function of temperature (T) in figure 1(a) and (b) respectively. The results clearly suggest insulating behaviour for these compounds. However, the transport does not follow a single activated dependence as illustrated in the insets, where we show the dependence of resistivity (ρ) on the temperature (T) in an $\ln \rho$ against $1/T$ plot. The insets show a simple activated behaviour at the high-temperature regime, while there is a considerable deviation for $T < 120$ K (i.e. $1000/T > 8.5$). In this low-temperature regime, the resistivity appears to be best described by the variable range hopping (VRH) mechanism [17], as illustrated in the insets by the linear dependence of $\ln \rho$ on $1/T^{1/4}$. Combining these two behaviours, we find that the experimental transport data are well described over the entire temperature range in terms of simultaneous contributions to the conductivity (σ) both by an activated process and variable range hopping in the form

$$\sigma = \sigma_{01} \exp\left[-E_g/2k_BT\right] + \sigma_{02} \exp\left[-\left(T_0/T\right)^{1/4}\right]. \tag{1}$$

The resulting best fit is shown by solid lines through the data points in the main figures over the entire temperature range. The activated gaps (E_g) obtained from the fits are about 0.12 eV for $LaVO_3$ and 0.10 eV for $La_{0.9}Ca_{0.1}VO_3$. It is to be noted here that this estimate of the transport gap is about one order of magnitude smaller than the intrinsic Mott–Hubbard

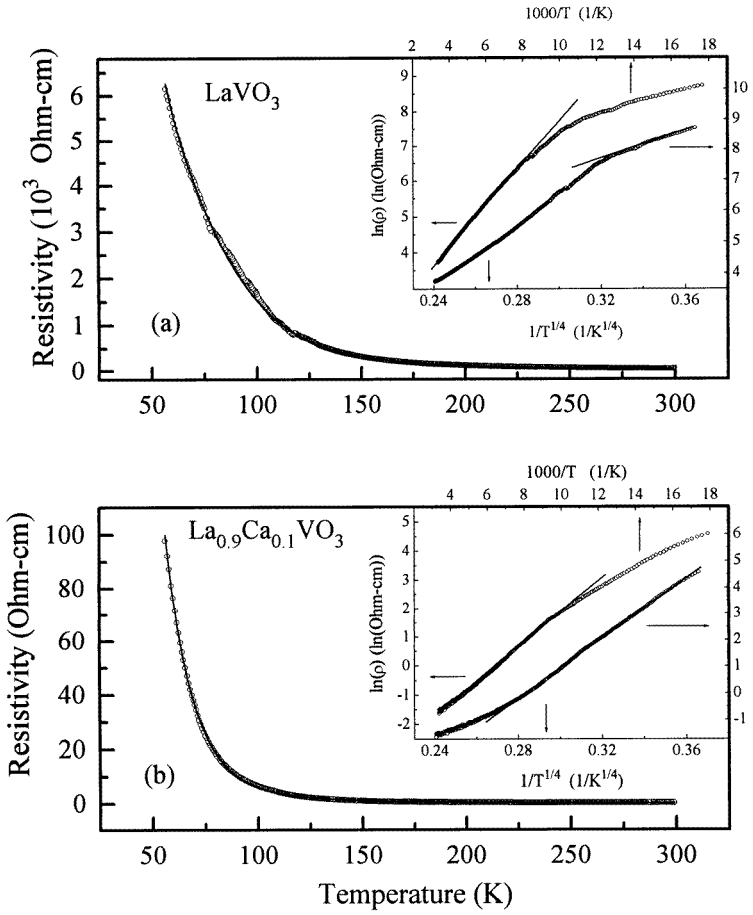

Figure 1. The resistivity (open circles) of (a) $LaVO_3$ and (b) $La_{0.9}Ca_{0.1}VO_3$ as a function of temperature. The solid lines show the best fit using the relation (1). The insets show the ln ρ against $1000/T$ and ln ρ against $1/T^{1/4}$ dependences.

gap (1.1 eV) in $LaVO_3$ estimated from optical spectroscopy [4]. We believe that the smaller activated gap arises due to the excitation to the localized doped hole states above the valence band arising from the non-stoichiometry observed in this system. The excitation across the intrinsic Mott–Hubbard gap barely contributes in the transport in this temperature range. The transport behaviour of $La_{0.9}Ca_{0.1}VO_3$ is very similar to that of $LaVO_3$, including very similar gaps in both the cases. However, the VRH appears to dominate over the activated behaviour over a wider range of temperature in $La_{0.9}Ca_{0.1}VO_3$. This suggests that Ca substitution generates hole states in an energy range similar to that introduced by oxygen non-stoichiometry in the parent compound. The larger extent of hole doping in the former, however, results in higher DOS at E_F, which are evidently localized due to disorder effects leading to a more extensive manifestation of VRH.

We show the resistivity as a function of temperature for the samples with $x = 0.2$, 0.3, 0.4 and 0.5 in figure 2. The plots clearly indicate metallic behaviour of these compositions, except for an upturn of resistivity with decreasing temperature below 100 K for $x = 0.2$ and 0.3 samples. Qualitatively, similar behaviour can also be observed in the case of

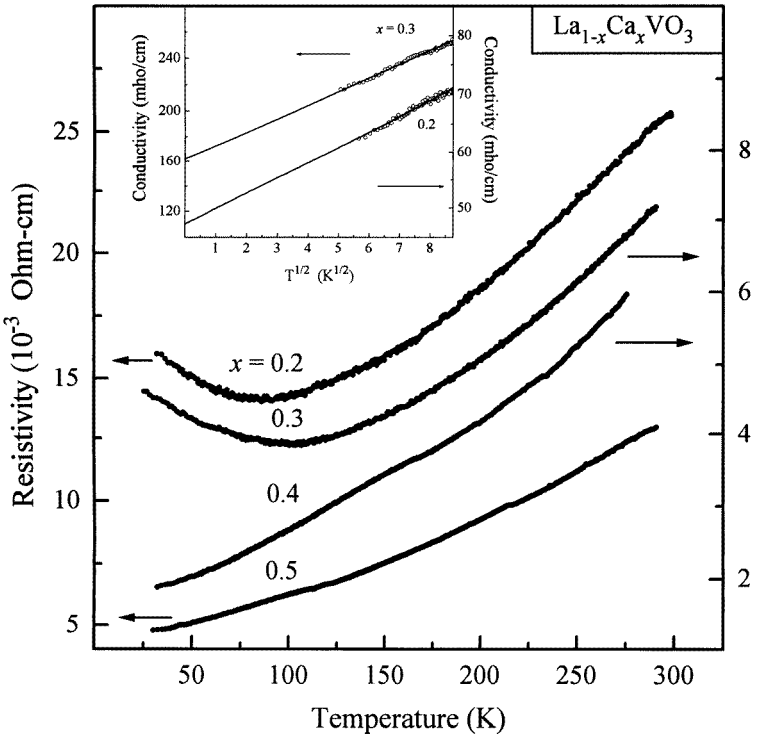

Figure 2. The resistivity of $La_{1-x}Ca_xVO_3$ for $x = 0.2$, 0.3, 0.4 and 0.5 as a function of temperature. The inset shows the $\ln\sigma$ against $T^{1/2}$ plots for $x = 0.2$ and 0.3 in the low-temperature region ($T < 100$ K).

$La_{1-x}Sr_xVO_3$ [4]. In spite of this increasing resistivity with decreasing temperature below 100 K, the $La_{1-x}Ca_xVO_3$ samples appear to have a finite $\rho(T \rightarrow 0\ \mathrm{K})$. This is better illustrated in the inset where we plot the conductivities of these two samples as a function of $T^{1/2}$ in the low-temperature region. These two plots suggest that the low-temperature conductivity $\sigma(T)$ is well described by the relationship $\sigma(T) = \sigma(0) + \beta T^{1/2}$, where $\sigma(0)$ is the finite conductivity at $T = 0$ K and the second term describes a square-root behaviour. Such a temperature dependence is well known in disordered metals in the presence of strong electron–electron interaction effects [17, 23, 24].

In order to investigate whether a Fermi liquid description is appropriate here, we analyse the resistivity of the metallic compositions in figure 3. These results clearly reveal a systematic behaviour with doping. The compositions for $x = 0.2$ and 0.3 are better described by T^2 dependence as observed in figure 3(a), while the conductivity at low temperature is dominated by the scattering at the impurity potentials for compositions close to the Mott transition with $T^{1/2}$ dependence (inset figure 2). These impurity potentials are well screened at higher temperature by the conduction electrons and the electron–electron interactions dominate in the resistivity giving rise to a T^2 dependence. Such behaviour is typical of a disordered Fermi liquid and thus, provides an example where the Mott transition can be described within the Fermi liquid description provided the effect of disorder is included. Compositions away from the Mott transition exhibit a considerable deviation from this behaviour. Larger carrier concentrations arising from higher doping, screen the impurity

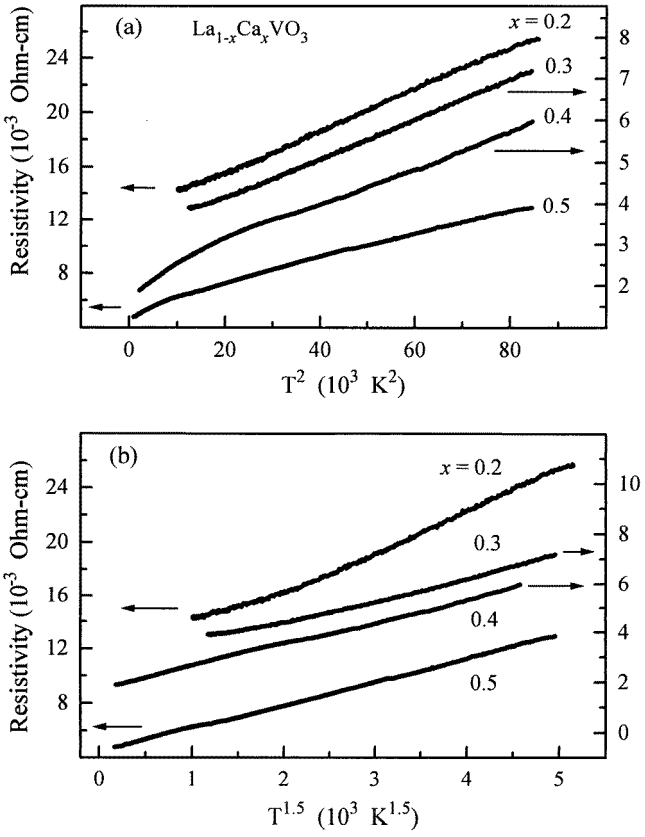

Figure 3. The resistivities of $La_{1-x}Ca_xVO_3$ for $x = 0.2$, 0.3, 0.4 and 0.5 as functions of (a) T^2 and (b) $T^{1/5}$.

potentials and consequently do not exhibit the $T^{1/2}$ dependence at low temperatures. Instead the resistivity over the entire range for $x = 0.4$ and 0.5 is better described by $T^{1.5}$ dependence as shown in figure 3(b) rather than a T^2 dependence (figure 3(a)). A recent observation on $La_{1-x}Sr_xVO_3$ [4] shows similar $T^{1.5}$ dependence over all the metallic compositions studied. In that study, this particular dependence for all the compositions has been attributed to spin fluctuation effects [25, 26]. If a similar mechanism is to be invoked in the present case, the $T^{1.5}$ dependence should be more clearly observable close to the antiferromagnetic to Pauli paramagnetic transition. In contrast, the resistivity is clearly better described by T^2 dependence for $x = 0.2$ and 0.3 (figure 3(a) and (b)) and the $T^{1.5}$ dependence manifests itself far away from the compositions for the magnetic transition, as shown later in the text. Therefore, the origin of this unusual $T^{1.5}$ dependence of resistivity is not clear at present.

We show the temperature dependence of magnetic susceptibility (χ) in figure 4. For $x = 0.0$ and 0.1 there is a maximum in the susceptibility, typical of an antiferromagnetic system; from these results, we obtain the Néel temperature for $LaVO_3$ to be around 125 K and that of $La_{0.9}Ca_{0.1}VO_3$ to be around 115 K. The further increase in susceptibility below T_N in the case of $La_{0.9}Ca_{0.1}VO_3$ may be due to the presence of localized isolated magnetic moments near the doped sites. For $x \geqslant 0.2$ the susceptibility is nearly independent of temperature except for an increase at the low temperatures. Such an increase in the magnetic

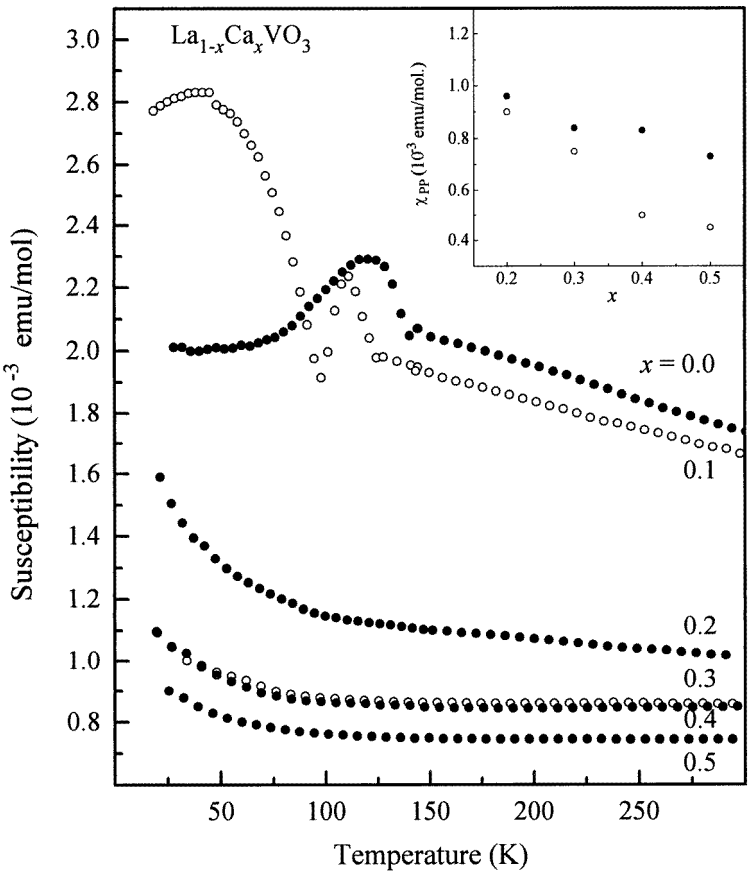

Figure 4. The magnetic susceptibility of $La_{1-x}Ca_xVO_3$ for $x = 0.0$, 0.1, 0.2, 0.3, 0.4 and 0.5. The inset shows the Pauli paramagnetic susceptibility in $La_{1-x}M_xVO_3$ (M = Ca (solid circles) and M = Sr (open circles)) for $x \geqslant 0.2$.

susceptibility at low temperature is associated with the presence of localized magnetic impurities, while the temperature independent component arises from Pauli-paramagnetism of the conduction electrons. The analysis based on these two contributions yields the Pauli paramagnetic part (χ_{PP}) to be 0.96, 0.84, 0.83 and 0.73×10^{-3} emu mol^{-1} for $x = 0.2$, 0.3, 0.4 and 0.5 respectively. Thus, there is a monotonic decrease in susceptibility with increase in x. Moreover, in every case, χ_{PP} appears to be enhanced by approximately a factor of two compared to the free electron value, suggesting the presence of correlation effects. We compare χ_{PP} of $La_{1-x}Ca_xVO_3$ (solid circles) obtained here with that of $La_{1-x}Sr_xVO_3$ (open circles) obtained from [18] as a function of x in the inset. It is seen that χ_{PP} drops considerably faster in the case of Sr substituted compounds. This would indicate that the $La_{1-x}Ca_xVO_3$ series is more strongly correlated as compared to $La_{1-x}Sr_xVO_3$ at any given level of hole doping, with χ_{PP} being less strongly enhanced in the latter series. This is likely to be related to the increasing bandwidth with increasing Sr substitution in that series. Thus, the effective mass of the quasiparticles in a Ca substituted compound will be considerably enhanced compared to the Sr doped case arising from larger effective correlation in the former.

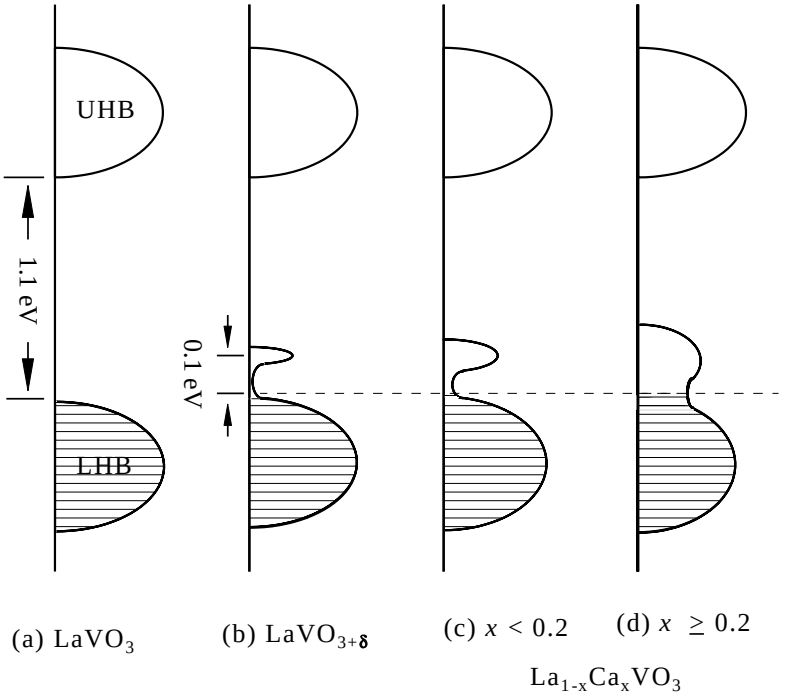

Figure 5. The schematic energy diagrams for $\delta = 0.0$ (a) $x = 0.0$, and for $\delta > 0.0$ (b) $x = 0.0$, (c) $x < 0.2$ and (d) $x \geqslant 0.2$ in $La_{1-x}Ca_xVO_{3+\delta}$.

On the basis of the present results we summarize the evolution of the electronic structure in $La_{1-x}Ca_xVO_3$ with composition as depicted schematically in figure 5. Figure 5(a) shows the schematic single-particle excitation spectra for both the occupied (lower Hubbard band (LHB)) and unoccupied (upper Hubbard band (UHB)) parts, separated by about 1.1 eV as suggested by optical measurements [4]. The presence of oxygen non-stoichiometry in normally prepared $LaVO_{3+\delta}$ introduces hole states about 0.1 eV above the top of the LHB as shown in figure 5(b); this evidenced by the activated transport with a characteristic gap of about 1.1 eV as shown in figure 1. The low-intensity tails of these states overlap the top of the LHB and thus, the Fermi energy, E_F, lies within a continuum of states. However, these low-density continuum states in the vicinity of E_F in figure 5(b) are localized due to disorder effects and thus lead to the VRH dominated $T^{1/4}$ dependence of conductivity at the lowest temperatures (see figure 1). Doping of Ca in place of La in $La_{1-x}Ca_xVO_3$ with $x < 0.2$ (figure 5(c)) appears to dope hole states further in a similar energy range as in the case of $LaVO_{3+\delta}$ (figure 5(b)), thus, exhibiting similar temperature dependent resistivities in both the samples (figures 1(a) and 1(b)). However, there are more continuum states at E_F in the presence of 10% Ca doping ($x = 0.1$) compared to $LaVO_{3+\delta}$; thus, VRH in the Ca doped case dominates over a wider temperature range. With further doping of Ca, the doped states become broader and more intense leading to a significant overlap with the LHB of the undoped compound. In this situation, the disorder effects are not strong enough to localize such high DOS and consequently the samples with $x \geqslant 0.2$ have a metallic ground state (figure 5(d)).

The authors thank G Kotliar for useful discussions. KM acknowledges the Council of Scientific and Industrial Research, Government of India, for financial assistance.

References

[1] Tokura Y *et al* 1993 *Phys. Rev. Lett.* **70** 2126
Kumagai K *et al* 1993 *Phys. Rev.* B **48** 7636
[2] Dougier P and Hagenmuller P 1975 *J. Solid State Chem.* **15** 158
[3] Mott N F *et al* 1975 *Proc. R. Soc.* A **345** 169
[4] Inaba F *et al* 1995 *Phys. Rev.* B **52** 2221
[5] Dougier P *et al* 1976 *J. Solid State Chem.* **19** 135
Nguyen H C and Goodenough J B 1995 *Phys. Rev.* B **52** 8776
[6] Kasuya M *et al* 1993 *Phys. Rev.* B **47** 6197
[7] Inoue I H *et al* 1995 *Phys. Rev. Lett.* **74** 2539
[8] McWhan D B *et al* 1971 *J. Physique* **32** C1 1079
Shivashankar S A and Honig J M 1983 *Phys. Rev.* B **28** 5695
[9] Mahajan A V *et al* 1992 *Phys. Rev.* B **46** 10 966
[10] Wold A and Ward R 1954 *J. Am. Chem. Soc.* **76** 1029
[11] Yakel H L 1955 *Acta Crystallogr.* **8** 394
[12] Dougier P and Casalot A 1970 *J. Solid State Chem.* **2** 396
[13] Shine-ike T *et al* 1976 *Mater. Res. Bull.* **11** 249
[14] Zubkov V G *et al* 1973 *Fiz. Tverd. Tela* **15** 1610 (Engl. transl. 1973 *Sov. Phys.–Solid State* **15** 1078)
[15] Ganguly P *et al* 1976 *Phys. Status Solidi* a **36** 669
[16] Reuter B and Wollnik M 1963 *Naturwissenschaften* **50** 569
[17] Mott N F 1994 *Metal—Insulator Transitions* (London: Taylor and Francis)
[18] Mahajan A V *et al* 1992 *Phys. Rev.* B **46** 10 973
[19] Kasuya M *et al* 1993 *Phys. Rev.* B **47** 6197
[20] Sawada H *et al* 1996 *Phys. Rev.* B **53** 12 742
[21] Shanon R D 1996 *Acta Crystallogr.* A **32** 751
[22] Fumitoshi I and Nishihara Y 1992 *J. Phys. Soc. Japan* **61** 1867
[23] Lee P A and Ramakrishnan T V 1985 *Rev. Mod. Phys.* **57** 287
[24] Altshuler B L and Aronov A G 1977 *JETP Lett.* **27** 664
[25] Moriya T 1985 *Spin Fluctuations in Itinerant Electron Magnetism* (Berlin: Springer)
[26] Ueda K 1977 *J. Phys. Soc. Japan* **43** 1497